J|A|C|S
ARTICLES
Published on Web 04/21/2004

Exchange Mechanisms for Sodium Dodecyl Sulfate Micelles: High Salt Concentration

Yahya Rharbi,† Liusheng Chen,‡ and Mitchell A. Winnik*

Contribution from the Department of Chemistry, University of Toronto, 80 St. George St., Toronto, Ontario, Canada M5S 3H6

Received August 4, 2003; E-mail: mwinnik@chem.utoronto.ca

Abstract: Solute exchange experiments for the pyrene-labeled triglyceride **TG-Py** solubilized in sodium dodecyl sulfate (SDS) micelles in the presence and absence of salt show that the "observed" rate constant k_{obs} for solute exchange varies by over 6 orders of magnitude as the free sodium ion concentration $[Na^+]_{aq}$ is varied between 10 and 850 mM. There is a sharp break in the log−log plot of k_{obs} versus $[Na^+]_{aq}$ in the range of $[Na^+]_{aq} = 200$ mM, with the exchange rate showing a weaker dependence on $[Na^+]_{aq}$ above this concentration. Up to 100 mM added NaCl, this exchange takes place essentially exclusively by a micelle fission mechanism in which each submicelle carries off one of the solutes. At higher salt concentrations, a bimolecular process becomes increasingly important. This fusion process, which involves formation of a transient supermicelle followed by fission back to two normal micelles, becomes the dominant process at high salt concentrations. The fission rate appears to level off for salt concentrations above 300−400 mM. These fission and fusion processes are related in an intimate way to the changes in the size and shape of the SDS micelles with increasing salt concentration.

Introduction

In this paper, we describe experiments which probe the influence of salt (sodium chloride) on the rate of solute exchange in sodium dodecyl sulfate (SDS) micelles. We focus on a range of salt concentrations near the transition from spherical micelles to rodlike assemblies. The solute is a water-insoluble pyrene derivative. The pyrene chromophore allows us to monitor solute exchange kinetics by a change in the excimer fluorescence emission intensity. The lack of water solubility means that solute exchange cannot occur by the exit−re-entry mechanism, in which the solute exits a micelle, diffuses through the aqueous medium, and re-enters a different micelle. Solute exchange can only occur by two alternative pathways. The first involves fission of a micelle into two submicelles, which subsequently grow back to proper (i.e., normal) micelles. The second mechanism involves fusion of two micelles to form a short-lived "supermicelle", which rapidly fragments back to two normal micelles. These two pathways have been invoked as mechanisms to explain the influence of salt on the rate of the slow relaxation pathway of SDS micelles as measured by traditional chemical relaxation kinetics measurements (pressure-jump, temperature-jump, stopped flow).[1] While these relaxation measurements provide precise values of the relaxation rates, one must resort to models to make inferences about the relaxation mechanism. Our experiments provide a direct measure of the rates of fusion and fission of SDS micelles.

Chart 1. (a) Exit-Re-entry Mechanism; (b) Collision−Exchange−Separation Mechanism; and (c) Fission−Growth Mechanism

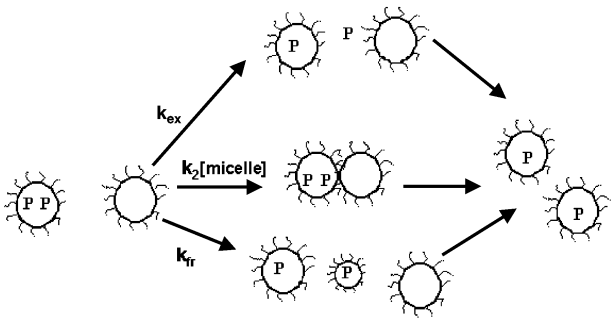

The three solute exchange mechanisms described above are shown schematically in Chart 1. We write this scheme for the case in which a micelle bearing two solutes (P) passes one of its solute molecules to a neighboring empty micelle. The top process (exit−re-entry) will exhibit first-order kinetics (rate constant, k_{ex}), because exit is rate limiting.[2−8] This process will

† Current address: Laboratoire de Rheologie, BP 53 − Domaine Universitaire, F-38041 Grenoble Cedex 9, France.

‡ Current address: Institute of Chemistry, The Chinese Academy of Sciences, Zhongguancun, Beijing 100080, China.

(1) For reviews of dynamic processes in micelles, see: (a) Muller, N. In *Solution Chemistry of Surfactants*; Mittal, K. L., Ed.; Plenum: New York, 1979; Vol. I, pp 267−295. (b) Gormally, J.; Gettins, W. J.; Wyn-Jones, E. In *Molecular Interactions*; Wiley: New York, 1980; Vol. 2, pp 143−177. (c) Lang, J.; Zana, R. In *Surfactant Solutions: New Methods of Investigation*; Zana, R., Ed.; Marcel Dekker: New York, 1987; pp 405−452. (d) Huibers, P. D. T.; Oh, S. G.; Shah, D. O. In *Surfactants in Solution*; Chattopadhay, A. K., Mittal, K. L., Eds.; Marcel Dekker: New York, 1995; Vol. 64, pp 105−121.
(2) Infelta, P. P.; Grätzel, M.; Thomas, J. K. *J. Phys. Chem.* **1974**, *78*, 190.
(3) Bolt, J. D.; Turro, N. J. *J. Phys. Chem.* **1981**, *85*, 4029.
(4) Almgren, M.; Grieser, F.; Thomas, J. K. *J. Am. Chem. Soc.* **1979**, *101*, 2021.
(5) Scaiano, J. C.; Selwyn, J. C. *Can. J. Chem.* **1981**, *59*, 2368.
(6) Selwyn, J. C.; Scaiano, J. C. *Can. J. Chem.* **1981**, *59*, 663.

be unimportant ($k_{ex} = 0$) if P is insoluble in water. The second process involves the collision of the two micelles in which exchange occurs either in a sticky collision accompanied by solute diffusion through the headgroup region or through transient fusion in which the micelle contents are randomized. This process will exhibit second-order kinetics (with rate constant, k_2). The third mechanism involves rate-limiting fission of the micelle (with rate constant, k_{fr}) in which each submicelle carries one of the probe molecules P.

Micelle Size and Shape. The presence of salt not only has a profound effect on the rate of micelle relaxation kinetics, but it also influences the size and shape of SDS micelles. This itself is a topic of great interest, as the references cited below attest. To place our own work in perspective, in the following paragraphs, we summarize some of the relevant information about SDS micelles.

In the absence of salt, SDS has a critical micelle concentration (cmc_o) of 8.3 mM. The cmc decreases in the presence of salt. An excellent discussion of this effect is given in the paper by Quina et al.[9] Based upon activity measurements, Sasaki et al.[10] found that the degree of dissociation of SDS micelles remained constant at $\alpha = 0.27$ in the range [SDS] = cmc to 80 mM. Aggregation numbers (N_{agg}) for SDS micelles as a function of surfactant and salt concentrations have been determined by small angle light and neutron (SANS) scattering, by ultracentrifugation, and by steady-state (SSFQ) and time-resolved fluorescence (TRFQ) quenching. In the vicinity of the cmc_o, N_{agg} is approximately 50.[11] These aggregation numbers increase with increasing surfactant concentration and in the presence of added salt.[12−16]

For salt concentrations up to about 0.2 M, there is good agreement in N_{agg} values obtained in different laboratories and by different techniques, with larger differences for values determined at higher salt concentration. Quina et al.[9] have argued that the key parameter describing the increase in N_{agg} is the concentration of free sodium ions $[Na^+]_{aq}$ in the aqueous medium, and they have shown that over a wide range of salt and SDS concentrations,

$$N_{agg} = \kappa_2([Na^+]_{aq})^{\gamma} \quad (1)$$

with $\kappa_2 = 162$ and $\gamma = 0.25$. The contributions to the free sodium ion concentration can be calculated via the conventional pseudophase ion exchange mass balance relationship.[9]

$$[Na^+]_{aq} = \alpha([SDS] - [SDS]_{free}) + [SDS]_{free} + [NaCl] = \alpha[SDS] + \beta[SDS]_{free} + [NaCl] \quad (2)$$

where [SDS] is the total surfactant concentration, $\beta = 1 - \alpha$, and $[SDS]_{free}$ is the concentration of free surfactant monomers in the solution. Bales et al.[15] provide an expanded discussion of this effect in the context of their electron spin resonance experiments on SDS micelles in the presence and absence of salt. They show that the hyperfine splitting parameter A_o is proportional to N_{agg} over a wide range of salt and surfactant concentrations. They argue that A_o can be determined with about 2 orders of magnitude better precision than N_{agg} itself. Defining $N_{agg} = \kappa_2(cmc_o)^{\gamma}$, Bales et al. show that their A_o values are consistent with the expression

$$N_{agg} = 50\left\{\frac{0.27[SDS] + 0.73[SDS]_{free} + [NaCl]}{0.0083}\right\}^{0.25} \quad (3)$$

For NaCl concentrations above 50 mM, $[SDS]_{free} \approx$ cmc. This analysis presumes that α is independent of the concentration of added salt over the entire concentration range of interest. Bales et al. find that the relationship between A_o and values of N_{agg} calculated in this way breaks down for N_{agg} greater than 120, corresponding most likely to a change in micelle shape to elongated structures.

For many years, scientists have assumed that the shape of SDS micelles at low ionic strength is spherical and that as the micelles grew in size with added salt, packing considerations would force the micelles to assume a more ellipsoidal shape.[17] A classic publication by Cabane et al.[18] described SANS experiments for salt-free solutions at 2 wt % (70 mM) surfactant concentration on SDS molecules selectively deuterated at specific sites. The authors concluded that, while the time-averaged shape of SDS micelles is spherical, the instantaneous shape is flattened and disklike. They infer that the micelle has a fluid structure and undergoes fluctuations between different disklike shapes. More recently, Bergström and Pedersen[19] reported detailed SANS experiments covering a much wider range of scattering vectors ($0.005 < q < 0.5$). They argued that simultaneous analysis of the high and low q region allowed for subtle discrimination between different models of SDS micelle shape. At low salt concentration, they deduced that SDS micelles were either oblate ellipsoids or torroidal disklike objects. For 0.5 wt % SDS (17 mM) at 40 °C in the absence of salt, they found that the micelles could be characterized as ellipsoids with half axes of a (height) = 13 Å, b (width) = c (length) = 23 Å, and an aggregation number of 54. We summarize these ideas about micelle shape and shape fluctuations in Figure 1. Because of limitations in our drawing software, there are sharp edges on the tabletlike disks we draw to represent the shape of micelles.

A matter of some controversy is the influence of the salt concentration on the distribution of micelle sizes. At low ionic strength, the size distribution is finite but narrow. The width of the distribution σ has been obtained as a fitting parameter in micelle relaxation kinetics experiments and from scattering experiments. As discussed in ref 18, several authors have

(7) Pileni, M. P.; Grätzel, M. *J. Phys. Chem.* **1980**, *84*, 1822.
(8) Hruska, Z.; Piton, M.; Yekta, A.; Duhamel, J.; Winnik, M. A.; Riess, G.; Croucher, M. D. *Macromolecules* **1993**, *26*, 1825.
(9) Quina, F. H.; Nassar, P. M.; Bonilha, J. B. S.; Bales, B. L. *J. Phys. Chem.* **1995**, *99*, 17028.
(10) Sasaki, T.; Hattori, M.; Sasaki, J.; Nukina, K. *Bull. Chem. Soc. Jpn.* **1975**, *48*, 1397.
(11) Bales, B. L.; Messina, L.; Vidal, A.; Peric, M.; Nascimento, O. R. *J. Phys. Chem. B* **1998**, *102*, 10347.
(12) For other studies of the influence of salt on the aggregation number of SDS micelles, see: (a) Warr, G. G.; Griesser, F. *J. Chem. Soc., Faraday Trans. I* **1986**, *82*, 1813−1828; 1829−1838. (b) Vass, Sz.; Török, T.; Jákli, Gy.; Berecz, E. *Prog. Colloid Polym. Sci.* **1988**, *76*, 221−223. Kratochvil, J. P. *J. Colloid Interface Sci.* **1980**, *75*, 271−275.
(13) Croonen, Y.; Geladé, E.; Van der Ziegel, M.; Van der Auweraer, M.; Vandendriessche, H.; De Schryver, F. C.; Almgren, M. *J. Phys. Chem.* **1983**, *87*, 1426.
(14) Almgren, M.; Swarup, S. In *Proceedings of the 4th International Symposium on Surfactants in Solution*; Mittal, K., Lindman, B., Eds.; Plenum: New York, 1984; Vol. 1, p 613.
(15) Bales, B. L.; Almgren, M. *J. Phys. Chem.* **1995**, *99*, 15153.
(16) Siemiarczuk, A.; Ware, W. R.; Liu, Y. S. *J. Phys. Chem.* **1993**, *97*, 8082.
(17) Israelachvili, J. N. *Intermolecular and Surface Forces*, 2nd ed.; Academic Press: London, 1991; Chapter 17.
(18) Cabane, B.; Duplessix, R.; Zemb, T. *J. Phys.* **1985**, *46*, 2161.
(19) Bergström, M.; Pedersen, J. S. *Phys. Chem. Chem. Phys.* **1999**, *1*, 4437.

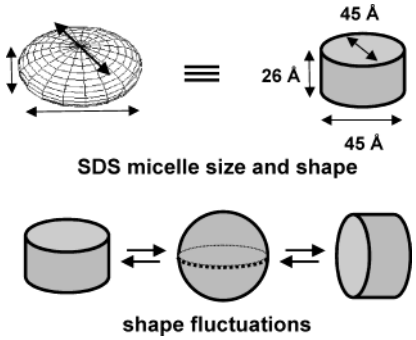

Figure 1. A representation of the size, shape, and shape fluctuations of SDS micelles in the absence of salt. We represent the oblate ellipsoid or torroidal micelle shape as a disk. The dimensions of the micelle come from SANS measurements at 40 °C as described in ref 19.

concluded from SANS measurements that, even at low salt concentrations, there is a significant polydispersity in micelle size.

Bergström and Pedersen comment that SANS data obtained over a limited range of scattering vectors can be fitted to a model of spheres with a significant standard deviation in the number-weighted size distribution, as well as to a model of monodisperse disklike objects. They find, at 40 °C for sodium bromide concentrations up to 0.5 M, that disklike objects with a narrow size distribution provide a better description of the full range of their data. In this range of salt concentrations, a broad distribution of micelle sizes was deduced by Siemiarczuk et al.[16] from TRFQ experiments analyzed as a distribution of lifetimes coupled with the maximum entropy method (MEM). Later, more extensive TRFQ experiments by Dutt et al.,[20] with data analyzed in terms of the traditional Tachiya−Infelta equation[21] coupled with global analysis, were consistent with a narrow SDS micelle size distribution,[22] particularly for 0.5 M NaBr. Hall[23] responded to these results with a theoretical analysis that supports the possibility of larger micelles maintaining a narrow size distribution. He showed that a narrow size distribution can be maintained if the "effective degree of micellar dissociation" α decreases with increasing aggregation number. This effect would be too small to detect from the effect of electrolyte on the cmc.

At higher salt and surfactant concentration, SDS micelles undergo a transition to form extended (wormlike) micelles.[24,25] High-resolution SANS experiments by Cabane[26,27] establish that long rodlike micelles are present at high salt concentration. Almgren et al.[28] used a combination of light scattering, SANS, and TRFQ to examine the properties of SDS in 800 mM NaCl for SDS concentrations ranging from 10 to 80 mM. At the lowest temperature (25 °C) and the highest surfactant concentration, they found short rodlike structures. The fluorescence quenching results are in agreement with a growth from globular to elongated micelles with a broad size distribution when the temperature is decreased from 45 to 25 °C. Deeper insights into the shape of these aggregates are provided by the more recent SANS measurements of Bergström and Pedersen,[19] which we will describe in more detail later in this paper.

Micelle Dynamics. When solutions of aqueous micelles such as SDS are subjected to a small perturbation from equilibrium, the subsequent relaxation is characterized by two well-separated relaxation times.[29] Aniansson and Wall[30] [AW] assigned the fast process, which occurs on a time scale of microseconds, to an association−dissociation process involving the exchange of individual surfactant molecules between the micelles and the water phase.[31] This process yields a change of the size of the micelles without affecting their number. AW attributed the slow process to the establishment of the equilibrium by a flux of aggregates through the minimum in the size distribution, which acts as the rate-determining region. The flux occurs through a sequence of surfactant monomer association or dissociation steps, which leads ultimately to the formation or breakdown of entire micelles. This process yields a change of both the size of the micelles and their numbers.

An important feature of the relaxation kinetics experiments with SDS is the finding that the slow relaxation rate ($1/\tau_{slow}$) decreases with increasing salt or surfactant concentration, and then crosses over to a new relaxation mechanism whose rate increases rapidly with [Na^+]. Lessner et al.[32] were able to account quantitatively for the rate decrease by modifying the AW analysis to accommodate the counterion contribution to micelle relaxation process for ionic micelles. They wrote for this process

$$N_{i-1} + N_1 + (j_i - j_{i-1})N_g = N_i \qquad (4)$$

where N_i denotes the number density of particles of class i, j_i is the number of undissociated monomers per particle, and N_g is the number density of counterions. N_1 denotes the number density of free surfactant monomers. For this mechanism, the growth reactions at the minimum of the size distribution are rate limiting because of the low concentration of submicellar aggregates in this region.

Above a counterion concentration of 60 mM, they found that the slow relaxation rate ceased to decline. A new process dominated the slow exchange, with a rate that exhibited a striking increase with increasing counterion concentration. Over the range of 60−300 mM, this rate increased as $1/\tau_{slow} \approx [Na^+]^y$, with $y = 6$. For this new pathway, they invoked a mechanism involving coagulation of submicellar aggregates. This process is written

$$N_k + N_l \underset{b_{kl}}{\overset{a_{kl}}{\rightleftharpoons}} N_i \qquad k + l = i \qquad (5)$$

where k and l denote a class of submicellar aggregates that associate with a rate a_{kl}, and i denotes a class of proper micelles.

(20) Dutt, G. B.; van Stam, J.; De Schryver, F. C. *Langmuir* **1997**, *13*, 1957.
(21) (a) Infelta, P. P.; Grätzel, M.; Thomas, J. K. *J. Phys. Chem.* **1974**, *78*, 190. (b) Infelta, P. P.; Grätzel, M. *J. Chem. Phys.* **1983**, *78*, 5280. (c) Tachiya, M. *Chem. Phys. Lett.* **1975**, *33*, 289. (d) Tachiya, M. *J. Chem. Phys*. **1982**, *76*, 340; **1983**, *78*, 5282.
(22) Almgren, M.; Lofroth, J.-E. *J. Colloid Interface Sci.* **1981**, *81*, 486.
(23) Hall, D. G. *Langmuir* **1999**, *15*, 3843.
(24) Hayashi, S.; Ikeda, S. *J. Phys. Chem*. **1980**, *84*, 744.
(25) Ikeda, S.; Hayashi, S.; Imae, T. *J. Phys. Chem*. **1981**, *85*, 106.
(26) Cabane, B. In *Surfactant Solutions: New Methods of Investigation*; Zana, R., Ed.; Surfactant Science Ser. 22; Marcel Dekker: New York, 1987; p 57.
(27) Cabane, B.; Duplessix, R.; Zemb, T. In *Surfactants in Solution*; Mittal, K. L., Lindman, B., Eds.; Marcel Dekker: New York, 1984; Vol. 1, p 373.
(28) Almgren, M.; Gimel, J. C.; Wang, K.; Karlsson, G.; Edwards, K.; Brown, W.; Mortensen, K. *J. Colloid Interface Sci*. **1998**, *202*, 222.
(29) Lang, J.; Tondre, C.; Zana, R.; Bauer, H.; Hoffmann, H.; Ulbricht, W. *J. Phys. Chem*. **1975**, *79*, 275.
(30) Aniansson, E. A. G.; Wall, S. N. *J. Phys. Chem*. **1974**, *78*, 1024−1030; **1975**, *79*, 857−858.
(31) Aniansson, E. A. G.; Wall, S. N.; Almgren, M.; Hoffmann, H.; Kielmann, H.; Ulbricht, W.; Zana, R.; Lang, J.; Tondre, C. *J. Phys. Chem*. **1976**, *80*, 905.
(32) (a) Lessner, E.; Teubner, M.; Kahlweit, M. *J. Phys. Chem.* **1981**, *85*, 1529; (b) **1981**, *85*, 3167.

They reasoned that, at low ionic strength, this mechanism would be suppressed because of the strong electrostatic repulsion between charged entities. As the ionic strength of the solution increased, the potential barrier between aggregates becomes so low that attractive dispersion forces can lead to coagulation.

For us, the interesting feature of the mechanism of eq 5 is the suggestion that normal micelles undergo spontaneous fission, where b_{kl} describes the rate of the reaction $i \rightarrow k + l$. In the notation of Lessner et al., β_i is the sum of fission rates of the proper micelles of class i, and β refers to the sum of fission rates summed over the distribution of proper micelles. These authors point out that β should be a function of the counterion concentration. The law of mass action requires the ratio a_{kl}/b_{kl} to be independent of this concentration; thus b_{kl} should have the same counterion dependence as a_{kl}.

Solute Exchange with a Water-Insoluble Pyrene Probe. We recently developed a new approach to study the slow relaxation processes of surfactant micelles in water. This technique is based on the general phenomenon of solute exchange in surfactant micelles, a topic itself of great interest.[33,34] In these experiments, we employ the pyrene-containing triglyceride **TG-Py** as the solute.[35−37] Solutions of **TG-Py**

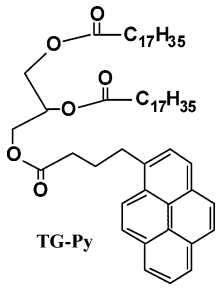

TG-Py

solubilized in nonionic surfactant micelles such as Triton X-100 (TX100) are easily prepared and exhibit a Poisson distribution of probes among micelles up to a mean occupancy of $\langle n \rangle = 2$ probes per micelle.[38] As in the case of other pyrene probes, micelles containing two or more molecules of **TG-Py** show a strong excimer fluorescence. When these solutions are treated with an excess of empty micelles, the excimer emission disappears as the probes exchange. In this way, we have learned that micelle fusion−fission is the dominant exchange pathway for nonionic micelles, but at low empty micelle concentration, the first-order contribution to the exchange rate can be measured.[36]

For the case of SDS micelles in the presence of added NaCl, we found that over the range of counterion concentrations for which $1/\tau_{slow}$ increases (60 mM < $[Na^+]$ < 150 mM), the exchange process follows first-order kinetics, with a rate constant k_{fr} that increases strongly as the counterion concentration is raised.[39,40] We argued that the new mechanism of micelle relaxation involved micelle fission into two "submicelles" as the rate-limiting step. From eq 5, it is easy to understand why values of k_{fr} are much smaller in magnitude than values of $1/\tau_{slow}$ determined by Lessner et al.[32] All values of b_{kl} contribute to $1/\tau_{slow}$, whereas only a small subset of fragmentation events are detected in the fluorescence experiment. These are the steps that yield two submicelles of sufficient size that both are able to transport a molecule of **TG-Py**.

In this paper, we examine the slow relaxation of SDS micelles at elevated salt concentration, covering a range of concentrations (up to 0.7 M) that includes the transition from globular (disklike) to extended wormlike micelles. Accompanying the change in micelle morphology, a new probe exchange mechanism takes over. This process exhibits second-order kinetics and likely involves micelle fusion followed by fission.

Experimental

Materials. The molecule **TG-Py** (M_w = 882) is a triglyceride in which 4-(1-pyrene)-butyric acid is one of the constituent fatty acid esters. Its synthesis and characterization is described elsewhere.[38] Ethyl pyrene was obtained from Molecular Probes (Eugene OR). Sodium dodecyl sulfate (SDS, Aldrich) and sodium chloride (NaCl, Aldrich) were used as received. Distilled water was further purified through a Millipore Milli-Q purification system.

Surfactant Solutions Containing Pyrene Derivatives. It is very difficult to dissolve hydrophobic probes such as **TG-Py** in aqueous solutions of SDS micelles. To prepare these solutions, we use an indirect method based on the ease of preparation of solutions of these probes **TG-Py** in aqueous Triton X-100 solution as described in ref 36. This transparent solution was diluted with aqueous TX100 surfactant solution and with water to yield a stock solution containing 0.50 g/L TX100 and ca. 4 μM of **TG-Py**. To 10 mL of this solution were added concentrated SDS solutions (10, 20, 30 g/L), and the mixture was stirred at room temperature for 1 h. Each final solution contains **TG-Py** at 0.20 μM and an initial SDS concentration of 21, 43, 65.7, and 86 mM. In all of these mixtures, TX100/SDS ≤ 1/350. The fluorescence emission of each mixture remained stable for a few days. The amount of **TG-Py** solubilized in each TX100 solution was determined by UV absorption measurements at 346 nm, using $\epsilon_{346} = 3.0 \times 10^4\ M^{-1}\ cm^{-1}$ determined previously.

Fluorescence Measurements. Static fluorescence measurements were carried out with a SPEX (2.1.2) Fluorolog spectrometer in the S/R mode. The signal intensity was kept below 2×10^6 counts/s to maintain the linearity of the detector response. For emission spectra and for time−scan kinetics experiments, λ_{ex} = 346 nm, whereas excitation spectra were obtained for both λ_{em} = 375 nm (monomer) and λ_{em} = 480 nm (excimer).

Kinetics Experiments. In measurements of the exchange kinetics, two solutions were mixed in the sample chamber of a home-built stopped-flow injector with a dead time of 2 ms.[40] In each injection, 0.35 mL of a solution containing [Py−R] in the range of 2.5 μM + SDS (0.68 mM) was mixed with 0.35 mL of a solution with [NaCl] varying from 0 to 300 mM. Experiments were carried out at room temperature, 23 °C. The signal was monitored at either λ_{em} = 375 nm or λ_{em} = 480 nm, with integration and interval times of 1 ms to 10 s and a total experiment time ranging from 1 to 10 000 s. In other experiments, solutions of **1** in [TX100] were mixed with [SDS] solutions in a similar fashion. Decay profiles were fitted to an exponential function or to a sum of two exponential terms.

Results

While it is straightforward to prepare solutions in which the probe **TG-Py** is dissolved in nonionic micelles such as those

(33) Barzykin, A. V.; Seki, K.; Tachiya, M. *Adv. Colloid Interface Sci.* **2001**, *89*, 47.
(34) Gehlen, M. H.; De Schryver, F. C. *Chem. Rev.* **1993**, *93*, 199.
(35) Rharbi, Y.; Winnik, M. A.; Hahn, K. G. *Langmuir* **1999**, *15*, 4697.
(36) Rharbi, Y.; Li, M.; Winnik, M. A.; Hahn, K. G. *J. Am. Chem. Soc.* **2000**, *122*, 6242.
(37) Rharbi, Y.; Winnik, M. A. *Adv. Colloid Interface Sci.* **2001**, *89*, 25.
(38) In these solutions, the probe **TG-Py** satisfies a Poisson distribution among micelles for values of $\langle n \rangle$ = 2.0. Rharbi, Y.; Kitaev, V.; Winnik, M. A.; Hahn, K. G. *Langmuir* **1999**, *15*, 2259−2266.
(39) Rharbi, Y.; Winnik, M. A. *J. Am. Chem. Soc.* **2002**, *124*, 2082.
(40) Rharbi, Y.; Winnik, M. A. *J. Phys. Chem. B* **2003**, *107*, 1491.

of Triton X-100 (TX100),[36,40] it is much more difficult to prepare solutions in which **TG-Py** is molecularly dissolved in SDS micelles. To overcome this problem, we followed an indirect approach reported originally by Dubin et al.,[41] in which a solution of **1** in TX100 was treated with a more concentrated solution of SDS. Individual surfactant molecules exchange rapidly to yield mixed micelles. With a sufficient excess of SDS, one obtains SDS micelles containing a trace of TX100 as an impurity. For example, under the conditions employed here at low salt concentration, we use such a large excess of SDS (typically 350-fold) that for $N_{agg} \approx 60$, only one micelle in five contains a TX100 molecule. The spectroscopic properties of pyrene probes in these micelles are identical to those of the probe in SDS micelles and very different from those in TX100 micelles.[40]

An important feature of this preparation methodology is that the probe itself does not become randomized among the micelles. The surfactant monomers exchange by the fast relaxation process. As Chart 1 emphasizes, if the probe molecules are insoluble in water, they can only exchange by one of the slow relaxation process involving micelle fusion or fission. Thus, the SDS micelles are created with a nonrandom (non-Poisson) probe distribution. The solution exhibits a measurable excimer emission, although if the probe were randomly distributed, the excimer fluorescence intensity would be too weak to be detected. A useful strategy for carrying probe exchange kinetics experiments is to mix the TX100 solution of **1** with an excess of SDS, and to use this mixture as a stock solution for subsequent experiments. When this solution is mixed, for example, with an equal volume of a concentrated NaCl solution, the solute exchange reaction is accelerated. Its rate can be monitored by the disappearance of the excimer emission, and the probe becomes randomized in the solution.

While the concentration of SDS in our experiments is known with high precision, determining the magnitude of rate constants requires knowledge of the micelle concentration in solution. The variation in the literature values of N_{agg} for SDS at high salt concentration prompted us to determine N_{agg} values using excimer formation from ethylpyrene under conditions very similar to those of our solute exchange experiments. Details of these experiments are provided as Supporting Information. To ensure confidence in the N_{agg} values obtained, we examined three concentrations of EtPy for each combination of salt and surfactant. Most experiments were carried out at [SDS] = 17.4 mM. For the two lowest salt concentrations (256 and 342 mM), we also examined solutions with [SDS] = 52.0 mM. Values of the aggregation numbers obtained in these experiments are listed in Table 1. We plot these values versus [NaCl] in Figure 2, where the line of smaller slope on the left-hand side of the graph approximates values obtained by others at lower salt concentrations. Examination of the fitting parameters leads to the conclusion that the micelle size distribution remains sufficiently narrow that the magnitude of the fitted probe lifetime τ_o and the intramicellar quenching rate constant k_Q were not measurably sensitive to the EtPy concentration. This conclusion is consistent with that drawn by Dutt et al.,[20] and the aggregation number we obtain for 0.51 M NaCl is similar to those (160−170) that they obtained at 0.50 M NaCl and at 0.475 and 0.545 M NaBr.

(41) Dubin, P. L.; Principi, B. A.; Smith, M. A.; Fallon, *J. Colloid Interface Sci*. **1989**, *127*, 558.

Table 1. Properties of SDS Micelles and of 1-Ethylpyrene in SDS Micelle Solutions in the Presence of Added Salt

[NaCl]/[SDS] mM	calculated cmc (mM)[a]	N_{agg}	$10^2 k_Q$, ns^{-1} [b]	$k_Q \times N_{agg}$, ns^{-1}	τ_o, ns[b]
256/17	0.68	143	2.54	3.64	122.4
342/17	0.55	141	2.61	3.68	125.0
428/17	0.47	164	2.12	3.47	125.2
513/17	0.41	176	1.62	2.86	123.9
684/17	0.33	215	0.78	1.68	117.0
256/52	0.68	142	2.43	3.45	122.9
342/52	0.55	143	2.40	3.43	128.1

[a] Calculated from the expression log(cmc) = −3.6 − 0.73 log[NaCl]. [b] The average of three values obtained at three different EtPy concentrations: k_Q is the pseudo-first-order quenching rate constant for excimer formation with the micelle; τ_o is the unquenched probe lifetime.

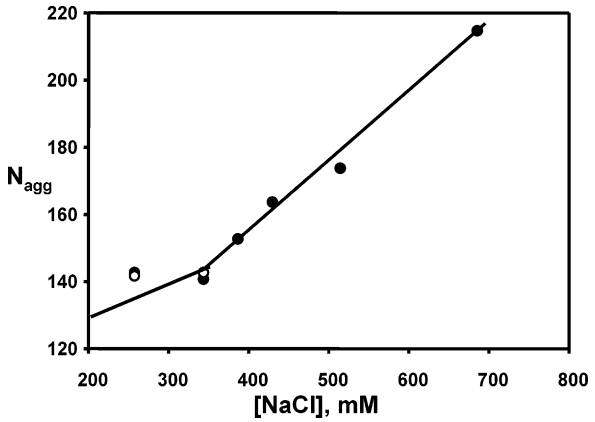

Figure 2. A plot of the mean aggregation numbers N_{agg} vs. [NaCl] for SDS concentrations of 17.4 mM (●) and 52.0 mM (○). The lines drawn are guides for the eye. The line of smaller slope is a reminder that the N_{agg} values show a smaller dependence on added salt at lower salt concentrations (cf., eq 3).

Solute Exchange Experiments. Solutions of **1** in SDS were prepared by the indirect route as described above. For relatively low concentrations of SDS (e.g., 17 mM), the fluorescence spectra were stable over several days. These solutions were then mixed in the sample chamber of a stopped-flow apparatus with an equal volume of an aqueous solution of NaCl. The initial solution exhibits a small but measurable excimer emission centered at 480 nm. When the system reaches equilibrium after mixing, the excimer emission is gone. A typical fluorescence spectrum is shown in Figure 3A. A typical time−scan experiment is shown in Figure 3B. In the discussion below, we ignore the small intensity changes that occur on a short time scale and focus on the exponential decay of the green "excimer" emission (I_E).[42] To avoid complications in the relaxation kinetics associated with three or more probes per micelle,[43] we prepared our SDS stock solutions from solutions of **1** in TX100 in which the average number of pyrene probes per micelle ($\langle n \rangle$) was less than or equal to 0.5.

In the slow relaxation process, the number of micelles bearing a pair of pyrenes, $P(t)$, decrease exponentially with time, characterized by a pseudo-first-order rate constant k_{obs}, which contains contributions from the various exchange processes described in Chart 1.

(42) The characteristic relaxation rates differ by at least a factor of 20. In ref 40, we assigned the fast response to a rearrangement of the micelles in response to the increase in counterion concentration. Here, as in those experiments, the slow response is due to solute exchange.

(43) Hilczer, M.; Barzykin, A. V.; Tachiya, M. *Langmuir* **2001**, *15*, 4196−4201.

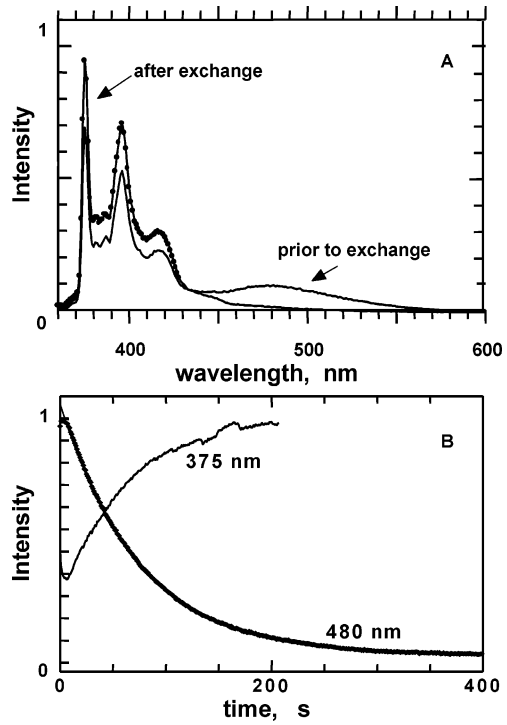

Figure 3. (A) Emission spectra (λ_{ex} = 346 nm) of **1** solubilized in aqueous solutions of SDS micelles. The spectrum labeled "prior to exchange" ([**1**] = 1.1 μM and [SDS] = 140 mM) refers to the freshly prepared sample. The spectrum "after exchange" refers to the spectra measured after 2 days. (B) Time−scan experiments monitoring the increase in I_M (λ_{em} = 375 nm) and the decrease in I_E (λ_{em} = 480 nm) after mixing a solution of **1** in SDS micelles ([**1**] = 1.1 μM, [SDS] = 80 mM) with an equal volume of NaCl solution ([NaCl]] = 0.2 M).

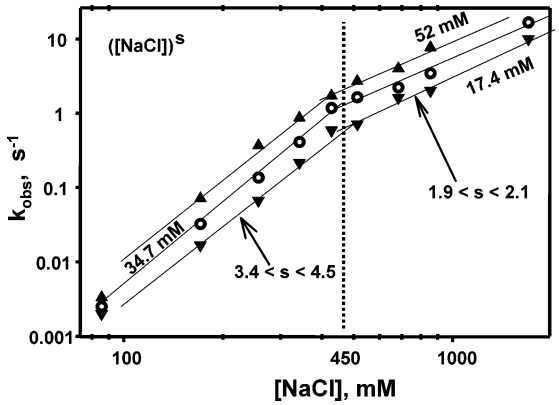

Figure 4. Log−log plots of k_{obs} versus [NaCl] for three different concentrations of SDS (17.4, 34.7, 52.0 mM). The I_E decays were measured following rapid mixing of a solution of **1** in SDS with an equal volume of NaCl solution. The solutions of **1** in SDS were prepared by mixing 5 wt % of a solution of **1** in TX100 (4 μM **1**, 0.5 g/L TX100) with 95 wt % of solutions of SDS (10, 20, and 30 g/L).

$$I_E \propto P(t) = P(0)\exp(-k_{obs}t) \qquad (6)$$

Solute exchange experiments were carried out over a wide range of salt concentrations for three different SDS concentrations (17.4, 34.7, and 52.0 mM). These data are presented in Figure 4, where we plot log k_{obs} versus log[NaCl]. Experiments at each of the three SDS concentrations show identical behavior: a steep powerlaw increase in rate up to [NaCl] = 0.45 M, crossing over to a much milder dependence at higher salt concentration. For both regimes, $k_{obs} \approx [NaCl]^y$, with y = 3.4−4.5 for the lower range of salt concentrations, and y = 1.9−2.1 for [NaCl] > 0.45 M.

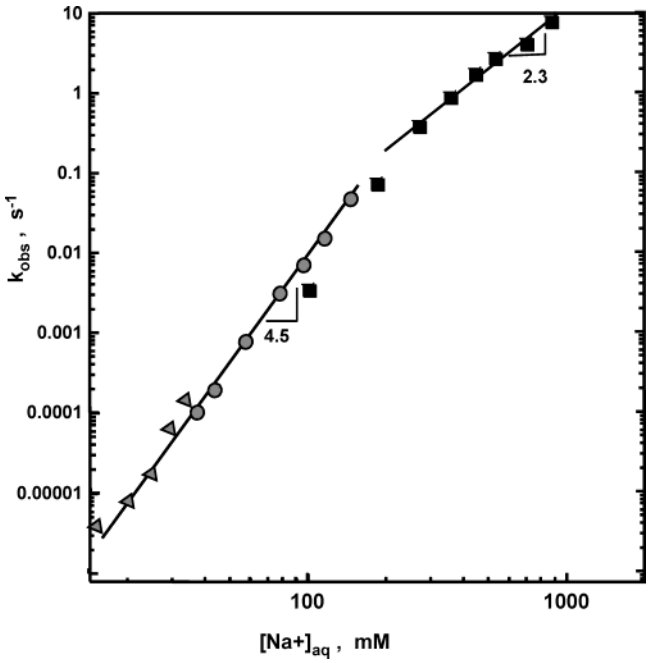

Figure 5. Log−log plot of k_{obs} versus $[Na^+]_{aq}$, combining results reported in ref 40 with data from Figure 4 for [SDS] = 52 mM.

Discussion

In a previous publication,[40] we demonstrated that solute exchange for **1** in SDS micelles is dominated by a first-order process involving fission−growth mechanisms for salt concentrations up to 140 mM. We reported that k_{obs} values increased by over 4 orders of magnitude as $[Na^+]$ was varied. In these experiments, the values of k_{obs} obtained by increasing the surfactant concentration in the absence of salt fit a common line with those obtained at an SDS concentration of 80 mM with [NaCl] increasing from 20 to 140 mM. To connect those experiments with the experiments described here, in Figure 5 we plot those data on a common graph with the data in Figure 4 for the highest SDS concentration. There appears to be a smooth crossover between the data obtained with [NaCl] < 200 mM, where k_{obs} increases as $[Na^+]^y$ with y = 4.5, to a high salt region with y = 2.3.

We would like to emphasize that this type of behavior is very unusual. It cannot represent a kinetic competition between two independent processes characterized by a different powerlaw dependence on $[Na^+]$. If this were the case, the mechanism with the stronger dependence would dominate at high salt concentration and not at low salt concentration. Whatever process is responsible for the exchange process characterized by y = 4.5, this process must reach a limiting value (or begin to decrease) in the range of 200 mM NaCl.

The second unusual aspect of the data in Figure 4 is the dependence of the solute exchange rate on surfactant concentration. We can distinguish three different regimes that show different behavior depending on the added salt concentration. In the absence of added salt, k_{obs} increases with surfactant concentration, but this effect is due only to the SDS contribution to the free sodium ion concentration. For experiments carried out at intermediate salt concentrations, for [NaCl] = 40−100 mM, k_{obs} exhibits almost no dependence on [SDS]. At higher salt concentrations, the data in Figure 4 show that k_{obs} values increase with SDS concentration. In ref 40, we described a set

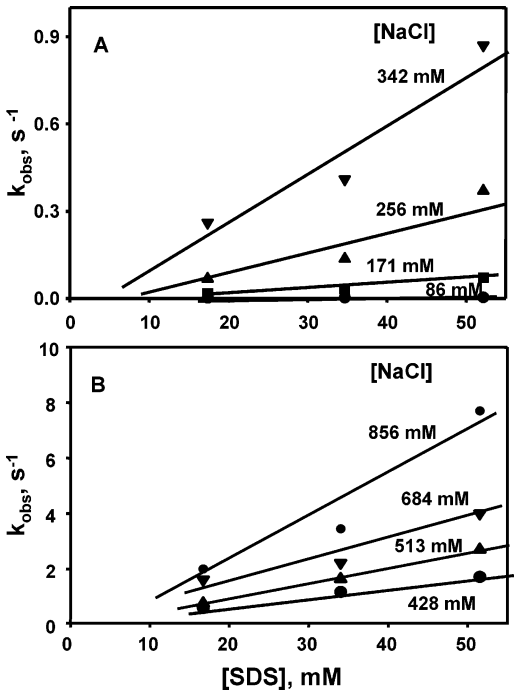

Figure 6. Plots of k_{obs} versus [SDS] for experiments carried out in the presence of NaCl. (A) Experiments at final concentrations of [NaCl] = 86, 171, and 256 mM. (B) Experiments at [NaCl] = 428, 513, 684, and 856 mM.

of experiments to examine the dependence of k_{obs} on SDS concentration, carried out at fixed salt concentration ([NaCl] = 140 mM). We found a weak increase of k_{obs} with increasing [SDS]. When these data were plotted as k_{obs} versus [micelle], we obtained a straight line with a small positive slope (38 M^{-1} s^{-1}) and an intercept of 0.037 s^{-1}. At that time, we were reluctant to attribute the positive slope to a second-order exchange process, because of the strong sensitivity of the first-order exchange rate to the $[Na^+]_{aq}$ concentration. The SDS added to the system also contributed to the free counterion concentration. To proceed with our analysis, we next consider how the exchange rate varies with [SDS] at elevated salt concentration.

Identifying the Exchange Mechanisms. Solute exchange can in principle occur by the three mechanisms indicated in Chart 1. For the case of **TG-Py** as the solute, its solubility in water is so low that $k_{exit} = 0$. Under these circumstances

$$k_{obs} = k_{fr} + k_2[\text{micelles}] = k_{fr} + k_2([\text{SDS}] - \text{cmc})/N_{agg} \quad (7)$$

The two solute exchange processes, fission−growth and fusion−fission, can be distinguished by their kinetic order. The former is characterized by first-order kinetics, whereas the latter will exhibit second-order kinetics.

To distinguish between these mechanisms, we carried out a series of solute exchange experiments varying the SDS concentration at constant salt concentration. Each of the experiments is characterized by a k_{obs} value that increases linearly with increasing [SDS]. The slopes increase in a striking manner with increasing salt concentration. In Figure 6A, we show the results for experiments carried our at [NaCl] = 86, 171, 256, and 342 mM. On this *y*-axis scale, the slope for the plot at [NaCl] = 86 mM is very small. At this low salt concentration, k_{obs} shows little dependence on surfactant concentration. The results from ref 42 for [NaCl] = 140 mM have a slope and intercept

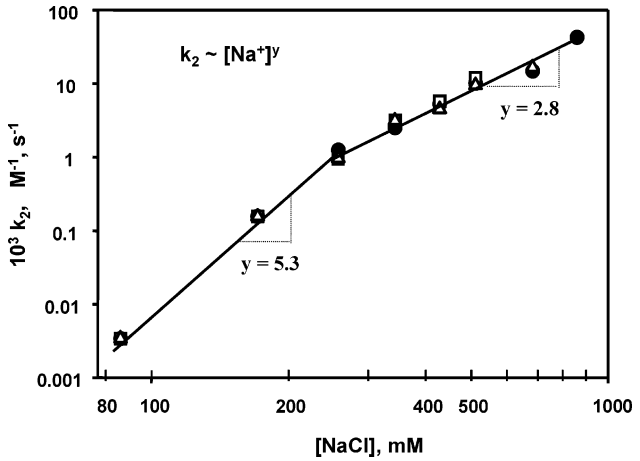

Figure 7. A log−log plot of k_2 versus [NaCl], in which the k_2 values were calculated from the plot of k_{obs} versus [micelle]. The micelle concentrations were calculated from the N_{agg} values in Table 1 (●), from ref 44 (□), and from ref 45 (△).

intermediate between those for 86 and 171 mM NaCl. The results for higher salt concentration are shown in Figure 6B. Here, the k_{obs} values also increase linearly with [SDS], and the slopes increase markedly with elevated salt concentration. These experiments establish that, in this range of salt concentrations, solute exchange occurs by a mechanism characterized by second-order kinetics.

According to eq 6, the rate constants for the competing first-order process are given by the magnitude of the intercepts obtained by extrapolating the plots in Figure 6 to [SDS] = 0. For [NaCl] < 80 mM, $k_{fr} = k_{obs}$, because the rates depend on surfactant concentration only through the SDS contribution to the over sodium ion concentration. For experiments carried out at 86 and 140 mM NaCl, the slopes in Figure 6A are so small that $k_{fr} \approx k_{obs}$, whereas for [NaCl] = 171, the intercept is close to the value of k_{obs} shown in Figure 5. For salt concentrations higher than 171 mM, it is difficult to comment on the influence of salt on the magnitude of the intercepts because the intercepts are within experimental error of zero.

To proceed more deeply with an analysis of the kinetic behavior of solute exchange at high salt concentration, we have to examine how the second-order rate constant k_2 depends on salt concentration. As indicated in eq 7, the micelle concentration is connected to the overall surfactant concentration through the micelle aggregation number. In the Introduction, we pointed out that for values of N_{agg} up to about 100−120, there is good agreement in the literature about the dependence of N_{agg} on sodium ion concentration. For experiments at higher salt concentration, the values of N_{agg} in the literature are more scattered. This was our motivation for determining values of N_{agg} on the basis of excimer formation by EtPy. Values of k_2 calculated using these N_{agg} values are plotted in Figure 7. As a check on these values, we also calculated values of k_2 using two extreme series of N_{agg} values found in the literature, from quasielastic light scattering,[44] and from TRFQ experiments involving methylpyrene with *m*-dicyanobenzene as the quencher.[45] Although these two reports describe a somewhat different

(44) Mazer, N.; Benedek, G.; Carey, C. *J. Phys. Chem.* **1976**, *80*, 1075.
(45) Croonen, Y.; Geladé, E.; Vabder Zegel, M.; Van der Auweraer, M.; Vanderdriessche, H.; De Schryver, F. C.; Almgren, M. *J. Phys. Chem.* **1983**, *87*, 1426.

dependence of N_{agg} on [Na^+] for [Na^+] > 350 mM, the calculated values of k_2 versus [Na^+] that we obtain using their N_{agg} values are very close to the values that we calculate with our N_{agg} values in Table 1.

The most striking feature of the data in Figure 7 is that for sodium ion concentrations up to 0.26 M, there is a steep increase in rate, which can be approximated as $k_2 \approx [Na^+]^{5.3}$. At higher salt concentration, the powerlaw behavior is more firmly established, with $k_2 \approx [Na^+]^y$, with $y = 2.8$. This exponent is larger than that ($y = 2.3$) seen for k_{obs} in Figure 5. This difference is a consequence of the fact that k_{fr} makes a more important contribution to k_{obs} at 200−300 mM NaCl than at higher salt concentrations.

There are subtle features of these data that require further comment. The slopes in Figure 6 are influenced by the contribution of SDS to the free sodium ion concentration. Thus, a fraction of the magnitude of the slope is due to the influence of increasing $[Na^+]_{aq}$ on the fission rate. Using the result in Figure 5 that $k_{obs} \approx [Na^+]_{aq}^{4.5}$, in conjunction with the finding that over most of this range of salt concentrations $k_{fr} = k_{obs}$, we can write $k_{fr} = k_{fr}^0[Na^+]_{aq}^{4.5}$, where k_{fr}^0 is a proportionality constant. Equation 7 can be rewritten

$$k_{obs} = 0.5k_{fus}[\text{micelles}] + k_{fr}^0[Na^+]_{aq}^{4.5} \quad (8)$$

Substituting the expression for $[Na^+]_{aq}$ (eq 2), we obtain

$$k_{obs} = 0.5k_{fus}[\text{micelles}] + k_{fr}^0(0.27N_{agg}[\text{micelles}] + \text{cmc} + [\text{NaCl}])^{4.5} \quad (9)$$

Here, we distinguish between the experimental values of k_2 obtained as the slopes of the plots in Figure 6 from the second-order fusion rate constant k_{fus} unaffected by the $[Na^+]_{aq}$ contribution to k_{fr}. The factor of 0.5 accounts for the reversibility of supermicelle formation. If one-half of the doubly occupied (P*/P) supermicelles formed in a fusion event undergo fission to form a doubly occupied micelle (return to starting material), the net rate of probe−quencher separation will be one-half the fusion rate.

At high salt concentration, the cmc is small. We can extract a factor of $[NaCl]^{4.5}$ from the second term in eq 9 and set $k_{fr} = k_{fr}^0[NaCl]^{4.5}$

$$k_{obs} = 0.5k_{fus}[\text{micelles}] + k_{fr}(0.27N_{agg}[\text{micelles}]/[\text{NaCl}] + 1)^{4.5} \quad (10)$$

Expanding the term in parentheses as a polynomial and keeping only the first-order term, we find

$$k_{obs} = 0.5k_{fus}[\text{micelles}] + 1.2[\text{micelles}] \times N_{agg} \times k_{fr}/[\text{NaCl}] + k_{fr} \quad (11)$$

$$k_{obs} = (0.5k_{fus} + 1.2N_{agg} \times k_{fr}/[\text{NaCl}])[\text{micelles}] + k_{fr} \quad (12)$$

Thus, in the presence of a fixed concentration of NaCl, the effect of a change in SDS concentration will appear as a second-order contribution ($k_2^{fr} = 1.2N_{agg}k_{fr}/[NaCl]$) to the observed exchange rate. For the lowest value of [NaCl] investigated, here 86 mM, $k_2^{fr} \approx 0.44 \times k_2$, and the real fusion rate $k_{fus} \approx 2 \times 0.56 \times k_2$. The contribution of k_2^{fr} to the measured solute exchange rate decreases with increasing [NaCl], because k_2^{fr} varies as [SDS]/[NaCl] (eq 12) and because k_{fr} tends to level off for [NaCl] > 300−350 mM. We estimate that beyond [NaCl] > 350 mM, k_2^{fr} is negligible, and $k_{fus} \approx 2k_2$.

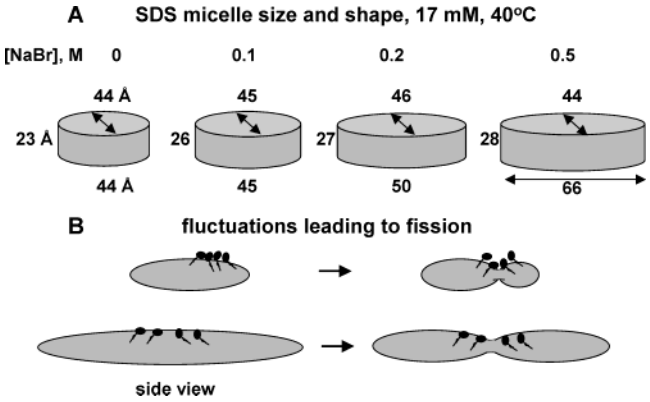

Figure 8. (A) The effect of NaBr concentration on the size and shape of SDS micelles as reported in ref 19. (B) A model showing how shape fluctuations lead to micelle fission.

Factors Affecting Micelle Fission and Fusion. In the preceding section, we established that, at low to modest sodium ion concentrations, SDS micelles undergo solute exchange by the fission−growth mechanism. This rate increases strongly with increasing salt concentration. Micelle fusion is undetectable for salt concentrations below 80 mM. A crossover occurs at higher salt concentrations, so that above 300 mM NaCl, solute exchange occurs almost exclusively by a second-order process. There are many interesting and unusual features about the crossover from fission- to fusion-dominated solute exchange. For example, at higher salt concentrations, the fission rate constant k_{fr} appears to reach a maximum value. To appreciate the factors that affect this change in mechanism, we need to consider how the counterion concentration affects the size and shape of SDS micelles.

Micelle Size and Shape. To appreciate how the micelle dimensions evolve in the presence of added salt, we refer to the SANS experiments of Bergström and Pedersen,[19] keeping in mind that their experiments were carried out at 40 °C, as compared to 25 °C for our measurements. They show that for each salt (NaBr) concentration they investigate, the SANS form factors for the micelles can be fitted to a model based on a monodisperse triaxial ellipsoid with a height of ca. 25 Å, a width of ca. 45 Å, and a length that increases with salt concentration. The best-fit dimensions for solutions at 0.5 wt % (17 mM) SDS are shown in Figure 8A. For [NaBr] = 0, 0.1, and 0.2 M, the dimensions are not sensitive to SDS concentration. At 0.5 M NaBr, the long axis increases from 64 to 67 to 72 Å as the SDS concentration is increased from 0.25 to 0.50 to 1.0 wt %. These correspond to $N_{agg} = 115$, 118, and 130, respectively.

The situation becomes more extreme at 0.7 M NaBr. Here, the data are best fitted by a flexible ribbonlike structure, polydisperse in length, with an ellipsoidal cross-section. For these samples, the thickness and width remain at ca. 25 and 40 Å, respectively. The mean length $\langle L \rangle$ and mean aggregation number $\langle N_{agg} \rangle$ increase with surfactant concentration, with respective values of $\langle L \rangle = 250$, 427, and 537 Å for SDS = 0.25, 0.50, and 1.0 wt %. These correspond to $\langle N_{agg} \rangle = 533$, 914, and 1184, respectively. It would be nice if we had similar data for SDS micelles at 25 °C. Unfortunately, no such data are available, and we can take advantage of this information in

only a qualitative sense. We know from the work of Almgren et al.,[28] who used a combination of scattering and TRFQ experiments to examine the influence of temperature on SDS micelles in the presence of 0.8 M NaCl, that the micelles are larger and more elongated at 25 °C than at 40 °C.

The structures inferred from SANS measurements have an appealing simplicity. To test the structures used as models to fit the scattering data, it would be useful in the future to carry out high-level molecular dynamics simulations. Only through simulations could one assess the contribution of dynamic fluctuations to the overall micelle shape. These fluctuations must play an important role in the fission and fusion processes that we describe in this paper.

Micelle Fission. For micelle fission into submicelles, large amplitude fluctuations are necessary. These must lead to local regions of negative curvature in the micelle structure, followed by a "pinching off" process that leads to two smaller aggregates. A drawing illustrating this process is shown in Figure 8B. In a previous publication, we explained the increase in k_{fr} with increasing salt concentration in terms of the influence of the counterion on the fluctuations that lead to fission. Two factors resist these fluctuations, a local effect associated with the sites of negative curvature, and a global effect related to the increase in interfacial area of the micelle. In the region of the local effect, the headgroups of the surfactant molecules are forced together, and headgroup proximity is opposed by electrostatic interactions. When the salt concentration is increased, the electrostatic repulsion between headgroups is screened. In addition, there is a net reduction in the effective headgroup size. Both factors help to lower the repulsion between headgroups and promote the fluctuations that lead to fission.

In this paper, we need to explain why the fission rate levels off at high salt concentrations. To appreciate this effect, consider the influence of salt concentration on the magnitude of k_{obs}. If the fission process followed the tendency $k_{fr} \approx [Na^+]_{aq}^{4.5}$ for all salt concentrations, it would reach a value of ca. 100 s^{-1} for $[Na^+] = 864$ mM.[46] This value is much higher than that of k_{obs} seen in Figure 5. Because k_{fr} represents only one of the mechanisms contributing to the magnitude of k_{obs}, fission must be of decreasing importance at high salt concentrations. It is likely that the fission process in SDS reaches a limiting value or a maximum value of <0.5 s^{-1} in the range of $[Na^+] \approx 300-400$ mM.

Experiments on nonionic micelles have shown that the fission rate is sensitive to the size or structure of the probe.[36] The presence of the probe in a micelle likely retards its fission rate. We proposed that, among the large spectrum of fission events, only those are observed that yield two submicelles large enough to bear the probe molecule. When a fission event produces a small and a large fragment, both probe molecules remain in the large one, and the event is not recorded. For the case of SDS micelles, this model explains the fact that chemical relaxation measurements yield much higher fission rates (>100-fold) than those found in our experiments. In ref 40, we proposed the idea that there is a minimum micelle size for which both submicelles are large enough to bear the hydrophobic probe. Upon addition of salt, the micelle size distribution shifts toward higher values of N_{agg}, accompanied by an increase in the fraction of micelles within the distribution that yield detectable fission events. For large values of N_{agg}, the number of fission events yielding partition of the probes between fragments would become insensitive to the shift in the micelle size distribution, and k_{fr} would become insensitive to further addition of salt.

This argument can be developed somewhat differently in terms of the structures in Figure 8. Increasing salt concentration leads to a decrease in headgroup size and a decrease in headgroup repulsion. As a consequence, micelle curvature is reduced, and elongated structures are formed. As the curvature along the long axis is reduced, there will be a smaller fractional increase in the interfacial area associated with fission. Further increase in the salt concentration will have a minimal influence on headgroup repulsion, and the decrease in headgroup size may even lead to an increase in micelle cohesion. These effects will reduce the influence of additional salt on the fission rate.

Micelle Fusion. On the simplest level, one understands that the interaction between ionic micelles is dominated by electrostatic effects and that double layer repulsion is responsible for the barrier to close approach of SDS micelles. According to DLVO theory, the interaction potential between two charged particles is the sum of the attractive van der Waals forces and the repulsive electrostatic forces. This potential exhibits a maximum (E_{max}) which decreases with an increase in the counterion concentration.[47] When E_{max} is substantially higher than kT, the particles are protected against aggregation and flocculation, and this same barrier will suppress exchange through micelle fusion. Addition of salt decreases the energy barrier E_{max}. As more salt is added, the magnitude of E_{max} will decrease to the point that close approach between micelles is possible, and solute exchange can occur through a fusion−fragmentation process. We have inferred that this process is immeasurably slow for salt concentrations below 80 mM. At 86, 140, and 171 mM salt, some solute exchange occurs by a second-order process. The k_2 values in Figure 7 span nearly 4 orders of magnitude. Nevertheless, these rates are very slow. The largest value of k_2 (ca. 10^5 M^{-1} s^{-1}) is still about 10^4 times smaller than that of diffusion controlled. For each of these salt concentrations, E_{max} is still significantly larger than kT.[48]

We suggest that the onset of the SDS micelle fusion reaction is associated with the extended ellipsoidal shape of the micelles. We depict this process in Figure 9. Two elliptical micelles overcome the energy barrier E_{max} to fuse to form a transient supermicelle with dimensions larger than the mean size of normal micelles at that salt concentration. Fusion is likely favored by an edge-on or end-on approach of the micelles, which would experience less electrostatic repulsion than approaches involving one or both of the faces of the micelles. The supermicelle formed undergoes shape relaxation followed by fission back to two normal micelles. In the process, there is an exchange of solutes.

We are unable at this time to explain the change in slope in the logarithmic plot of k_2 versus [NaCl]. We may speculate, for example, that there is a minimum size for micelles that can undergo fusion. For salt concentrations less than 100 mM, only

(46) This value is also an order of magnitude larger than the value reported for the fission rate of Triton X-100 micelles.[36]

(47) Reference 17, pp 246−250.

(48) Solute exchange experiments at 25 °C with micelles of the nonionic surfactants Triton X-100 (an ethoxylated octylphenol with $N_{agg} = 100$) and Synperonic A7 (an ethoxylated mixture of linear C13 and C15 primary alcohols with $N_{agg} \approx 300$) gave k_2 values, respectively, of 1.5×10^6 and 9×10^4 M^{-1} s^{-1}. Rharbi, Y.; Bechtold, N.; Landfester, K.; Salzman, A.; Winnik, M. A. *Langmuir* **2003**, *19*, 10−17.

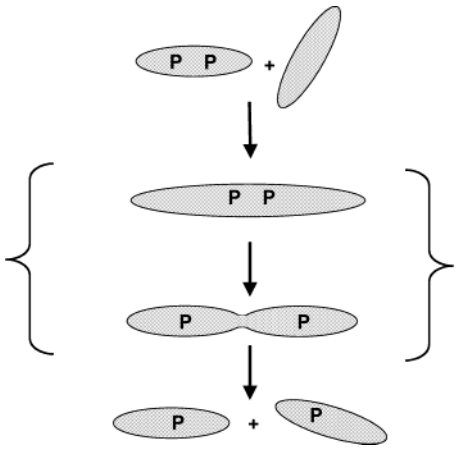

Figure 9. A model for the fusion (and solute exchange) of two oblate ellipsoidal micelles. The micelles collide and coalesce to form a short-lived supermicelle, which then fragments back to two normal micelles.

a tiny fraction of the micelle distribution may have this size. With increasing salt concentration, the increase in mean aggregation number will be accompanied by an increasing fraction of the micelles large enough to undergo fusion. This effect would eventually level off. The remaining increase ($k_2 \approx [Na^+]_{aq}^{2.8}$) is due to other factors, such as changes in micelle shape and reduction in the electrostatic barrier to fusion. A more precise explanation will require more detailed information about the size, shape, and surface charge of the micelles at each of the salt and surfactant concentrations in our experiments.

Summary

Solute exchange experiments for the pyrene-labeled triglyceride **TG-Py** solubilized in SDS micelles in the presence and absence of salt show that the rate constant k_{obs} for solute exchange varies by over 6 orders of magnitude as the free sodium ion concentration is varied between 10 and 850 mM. The kinetics show two regimes of powerlaw behavior $k_{obs} = [Na^+]_{aq}^{y}$ with $y = 4.5$ for $[Na^+]_{aq}$ up to 200 mM and $y = 2.3$ for the higher range of salt concentration. Up to 100 mM added NaCl, this exchange takes place almost exclusively by a micelle fission mechanism in which each submicelle carries off one of the solutes. The weaker dependence on $[Na^+]_{aq}$ at high salt concentration is an indication that the fission rate levels off for salt concentrations above 300−400 mM.

At high salt concentrations, a bimolecular process (with second-order rate constant k_2) becomes increasingly important and is the dominant mechanism for solute exchange at $[Na^+]_{aq} > 300$ mM. This fusion process involves formation of a transient supermicelle followed by fission back to two normal micelles. The fusion rate itself has a complex dependence on the sodium ion concentration. Changes in the fission rate can be rationalized in terms of changes in the micelle size and shape with increasing salt. The onset of micelle fusion at high salt concentrations is certainly promoted by a reduction of the electrostatic repulsion between micelles. It also likely related to changes in micelle size and shape, but how these operate to enhance the rate of micelle fusion remains to be elucidated.

Acknowledgment. The authors thank ICI, ICI Canada, and NSERC Canada for their support of this research. We also thank B. Cabane, M. Almgren, and F. Quina for helpful and thought-provoking discussions.

Supporting Information Available: Experimental details (PDF). This material is available free of charge via the Internet at http://pubs.acs.org.

JA0304805